Building ubiquitination machineries

Ramachandran, Sarath; Ciulli, Alessio

Published in:
Current Opinion in Structural Biology

DOI:
10.1016/j.sbi.2020.10.009

Publication date:
2021

Available online at www.sciencedirect.com

ScienceDirect

Current Opinion in Structural Biology

Building ubiquitination machineries: E3 ligase multi-subunit assembly and substrate targeting by PROTACs and molecular glues

Sarath Ramachandran and Alessio Ciulli

E3 ubiquitin ligase machineries are emerging as attractive therapeutic targets because they confer specificity to substrate ubiquitination and can be hijacked for targeted protein degradation. In this review, we bring to focus our current structural understanding of E3 ligase complexes, in particular the multi-subunit cullin RING ligases, and modulation thereof by small-molecule glues and PROTAC degraders. We highlight recent advances in elucidating the modular assembly of E3 ligase machineries, their diverse substrate and degron recognition mechanisms, and how these structural features impact on ligase function. We then outline the emergence of structures of E3 ligases bound to *neo*-substrates and degrader molecules, and highlight the importance of studying such ternary complexes for structure-based degrader design.

Address
School of Life Sciences, University of Dundee, Division of Biological Chemistry and Drug Discovery, James Black Centre, Dow Street, Dundee DD1 5EH, United Kingdom

Corresponding author: Ciulli, Alessio (a.ciulli@dundee.ac.uk)

Current Opinion in Structural Biology 2021, **67**:110–119

This review comes from a themed issue on **Macromolecular assemblies**

Edited by **Piero Crespo** and **Kylie Walters**

https://doi.org/10.1016/j.sbi.2020.10.009

Introduction

The ubiquitin–proteasome system (UPS) regulates protein homeostasis and is garnering increasing attention as a therapeutic target owing to its role in several diseases including cancer and neurodegeneration [1]. The post-translational addition of ubiquitin to substrate proteins is carried out sequentially by a cascade of three enzymes: E1-activating enzyme, which activates ubiquitin (Ub) in an ATP-dependent manner; E2-conjugating enzyme, to which the activated Ub is transferred via trans-esterification reaction; and E3 ubiquitin ligase, which catalyses the transfer of Ub from the E2 to a lysine residue on the substrate trough an isopeptide bond [2,3], although esterification reactions, for example, on threonine residues have been also reported [4].

E3 ubiquitin ligases can be branched into three classes: homologous to E6-AP C-terminus (HECT), really interesting new gene (RING) and RING-between-RING (RBR) ligases [5]. HECT E3s accept ubiquitin (Ub) from E2∼Ub to form a covalent thioester intermediate before transferring it on to the substrate [6]. In contrast, RING E3s brings E2∼Ub and substrate in close proximity to each other to mediate a direct transfer of ubiquitin to the substrate. The RBRs combine features of both HECT and RING families, as the N-terminal RING domain first recruits E2∼Ub conjugates and then transfers ubiquitin on to a HECT-type C-terminal catalytic cysteine residue before the final transfer on to the substrate [7]. Anaphase-promoting complex (APC/C) is a large (∼1.2 MDa) assembly of 11–13 proteins including a cullin (Apc2) and RING (Apc11) subunit, and regulates different stages of the cell cycle [8,9].

E3 ligases play a central role in imparting specificity to substrate recruitment. E3 ligase ubiquitination activity on native substrates is exquisitely controlled and regulated by protein–protein interactions (PPI) dictating their structural assembly. Furthermore, small-molecule degraders such as molecular glues and proteolysis-targeting chimeras (PROTACs) mediate recruitment of non-native interacting proteins to E3 ligases, thus hijacking the E3 intrinsic catalytic activity towards *neo*-substrates for proteasomal degradation. Here we review recent advances in elucidating the structural basis of building and hijacking ubiquitination machineries, with a focus on Cullin RING E3 ligase assembly, substrate recognition, and substrate recruitment mediated by degraders that holds attractive therapeutic potential.

Structural assembly and activity of modular multi-subunit E3 ligases

Cullin RING E3 ubiquitin ligases (CRLs) represent the largest family of E3 ligases. They are modular in that they are composed of an interchangeable substrate receptor, adaptor subunit(s), and a RING-box domain subunit, assembled around a central cullin scaffold subunit. CRLs are classified based on the type of cullin subunit (Cul1, Cul2, Cul3, Cul4A, Cul4B, Cul5 and Cul7) [10]. Structures of fully assembled CRL complexes have

highlighted a range of conformations and orientations attained by the different cullin subunits [11].

The crystal structure of $CRL2^{VHL}$ complex, composed of Cul2, RING-box protein (RBX1), Elongin B, Elongin C, and von Hippel-Lindau protein (VHL) highlights an inherent interdomain bending in Cullin scaffold proteins; allowing the cullin C-terminal globular domain and the N-terminal helical bundles domain to come closer in space when compared to previously reported CRL structures (Figure 1a) [12]. The structure also captures the RBX1 RING domain in an intermediate step in the full trajectory between inactive state and state activated by post-translational modification with the ubiquitin-like protein NEDD8 (neural precursor cell expressed developmentally downregulated protein 8) [12].

A recent cryo-electron microscopy structure captured a snapshot of a stable intermediate state of neddylated CRL en-route to substrate ubiquitination, providing

Figure 1

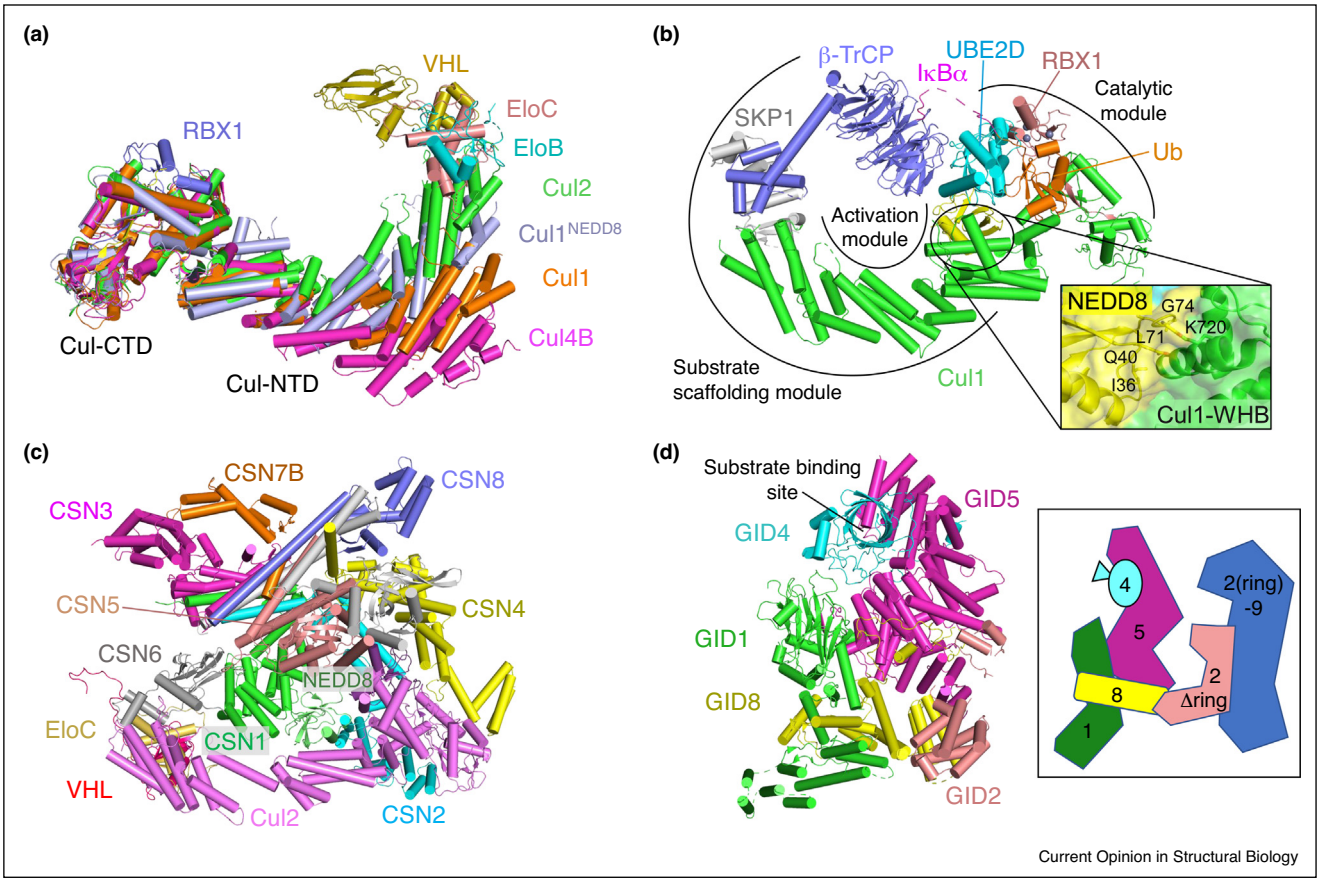

Structural assembly of modular multi-subunit E3 ligases: (a–d) Cartoon representation of each E3 ligase subunits with helices shown as cylinders. **(a)** E3 CRL assembly. Structural superposition of Cul2 (green, PDB: 5N4W [12]), NEDD8-modified Cul1 (light blue, PDB: 6TTU [13••]), CAND1-bound Cul1 (orange, PDB: 1U6G [59]) and Cul4B (magenta, PDB: 4A0L [60]) along the C-terminal domain (CTD) of Cul2 (residues 386–745) highlights the flexibility of Cullin subunits. For $CRL2^{VHL}$, ElonginB and RBX1 subunits bound to Cul2 are shown in cyan and slate, respectively. VHL (olive) from PDB: 1VCB [61] is superposed on PDB: 5N4W to show its location. For clarity only the cullin subunit is shown for the other CRL structures. **(b)** NEDD8 (yellow)-activated $CRL1^{β\text{-}TrCP}$–UBE2D∼Ub–IκBα substrate intermediate (PDB: 6TTU [13••]), in which UBE2D∼Ub is activated and juxtaposed with the substrate. Zoomed section shows the isopeptide bond between the terminal glycine of NEDD8 (yellow) and K720 of Cul1 (green) winged-helix B (WHB), activating the CRL. β-TrCP (slate), SKP1 (grey), and Cul1 (green) contribute as substrate scaffolding module presenting the IκBα (magenta)-bound β-TrCP to the catalytic module. The catalytic module is composed of UBE2D(cyan)∼Ub(orange)–RBX1 (wheat) in the canonical closed activated conformation. **(c)** Macromolecular structure of CSN–CRL2–NEDD8 (PDB: 6R7F [14•]). CRL2-NEDD8 components: Cul2 (violet), ElonginC (light orange), VHL (red) and NEDD8 (pale green). CSN2 (cyan) and CSN4 (yellow) clamp the Cul2 (violet) releasing the heterodimer composed of CSN5 (wheat) and CSN6 (grey), followed by deneddylation by CSN5. CSN3, CSN7B and CSN8 subunits are shown in magenta, orange and slate, respectively. **(d)** Multi-subunit GID E3 assembly: GID4 (cyan) acts as the substrate receptor, substrate binding site highlighted; GID1 (green), GID5 (magenta) and GID8 (yellow) act as scaffolding module; GID2 (wheat) and GID9 act as catalytic module. GID9 and GID2 ring domain is not modelled in the structure (PDB: 6SWY [21••]). Schematic diagram of the GID complex in the right shows the overall architecture of the assembly.

insights into the mechanism of NEDD8-mediated CRL activation. The structure comprises of neddylated CRL1$^{\beta\text{-TRCP}}$, ubiquitin-loaded E2 ubiquitin-conjugating enzyme UBE2D, and a phosphorylated peptide from IκBα (nuclear factor of kappa light polypeptide gene enhancer in B-cells inhibitor, alpha) (Figure 1b) [13••]. The full structure captures three distinct modules. First, NEDD8 is covalently linked to the winged helix-B (WHB) domain of cullin to form a globular activation module. Second, the catalytic module consists of ubiquitin-bound UBE2D and the RING domain of RBX1. Third, a so-called 'substrate-scaffolding module' comprising substrate receptor β-TRCP, adaptor subunit S-phase kinase-associated protein 1 (SKP1), and Cul1 together presents the β-TrCP-bound IκBα substrate towards the catalytic module. The mobile WHB domain of Cul1 permits the activation module to form multiple contacts between the 'backside' of UBE2D in the catalytic module and Cul1 in the substrate-scaffolding module. These extensive interactions facilitate the catalytic centre of UBE2D to be placed in proximity to the β-TRCP-bound substrate for subsequent ubiquitination.

Like ubiquitination, neddylation is also a reversible process. The deneddylation process is catalysed by the COP9 signalosome (CSN), an eight-subunit protein complex. A recent cryo-EM structure of the CSN tightly bound to neddylated CRL2$^{\text{VHL}}$ adds to the structural details from the previous structures of CSN interaction with CRL1, CRL3 and CRL4A (Figure 1c) [14•,15,16]. The structure reaffirms the conserved activation mechanism of the deneddylation machinery, including conformational clamping of CRL2 by CSN2/CSN4, release of the catalytic CSN5/CSN6 heterodimer, and subsequent activation of the metalloprotease CSN5 [14•]. More recently, inositol hexakisphosphate (IP6) has been characterized as a CSN cofactor that enhances interaction between CSN2 and RBX1, mediating CSN sequestration of CRL4 from UBE2R to prevent CRL4 activation [17•].

The eukaryotic N-end rule pathway was traditionally classified into the Arg/N-end rule (recognising N-terminal basic/bulky/arginylated Asp and Glu residues) pathway and the Ac/N-end rule pathway (recognising N-terminal acetylated residues) [18]. Glucose-induced degradation subunit 4 (GID4) represents the subunit of GID assembly ubiquitin ligase that recognises substrates harbouring a recently identified third branch of N-end degron, Pro/N-degrons [19•]. GID is a multisubunit E3 ligase from yeast that recognises the N-terminal proline of gluconeogenic enzymes and catalyses their ubiquitination (Figure 1d) [20]. The GID assembly assumes an anticipatory state GID$^{\text{Ant}}$ under carbon stress. With carbon recovery, glucose-induced expression of Gid4 transitions GID$^{\text{ant}}$ into active GID$^{\text{SR4}}$ recognizing isocitrate lyase (Icl1), fructose -1,6-bisphosphatase (Fbp1), and malate dehydrogenase (Mdh2) substrates [21••]. The role of different subunits in GID assembly can be clustered as catalytic module (GID2 and 9), scaffold module (GID1,8 and 5) and substrate receptor module (GID4 or 10). The eight β strands and four loops of GID4 β-barrel forms a narrow opening with the N-terminal proline filling snugly in the central cavity (Figure 2a). The selectivity for proline recognition is imparted by a tight network of hydrogen bonds and hydrophobic interactions [19•]. GID10 is proposed to be a substrate receptor that is expressed only under osmotic stress, although its substrate remains to be identified.

Substrate recognition by E3 ligase substrate receptors

CRLs employ a substrate receptor module to provide specificity for substrate recognition [10,11,22]. This section focuses on recent advances in the understanding of the structural basis of the highly diverse substrate recognition by E3 CRLs. The CRL1$^{\text{FBXL5}}$ — iron regulatory protein 2 (IRP2) complex structure provides insight into the oxygen sensing role of the [2Fe2S] cluster in binding to IRP2 (Figure 2b) [23•]. [2Fe2S] acts as a cofactor by forming coordination bonds with the conserved cysteines of F-Box and Leucine Rich Repeat Protein 5 (FBXL5), presenting the 'interface loop' of leucine rich repeat (LRR) domain to IRP2 domain IV [23•].

The CRL2 subunit Kelch domain-containing protein 2 (KLHDC2) was recently found to recognise substrates via a novel C-end degron protein-degradation mechanism, named DesCEND (destruction via C-end degron) [24,25••]. The crystal structure of KLHDC2 in complex with C-terminal diglycine degrons of early terminated selenoproteins SelK and SelS, and N-terminal proteolytic fragment of USP1 reveals a deep and basic pocket at the centre of the Kelch domain of KLHDC2 that recognises the substrate via a network of hydrogen bonding interactions with its terminal carboxyl group, achieving nanomolar binding affinities (Figure 2c) [24].

Unlike other cullins, CRL3 substrate receptors harbour substrate binding domain [kelch, or meprin and TRAF homology (MATH)] and adaptor domain [bric-a-brac/tramtrack/broad complex (BTB)] in a single polypeptide. Kelch-like protein 12 (KLHL12) and Kelch-like protein 20 (KLHL20) belong to substrate receptors with a Kelch domain. Two recent studies on KLHL12 characterize 'PGXPP' as the degron motif from substrate protein Dishevelled (Figure 2d) [26,27]. The structures reveal a U-shaped turn conformation of bound substrates in the KLHL12 hydrophobic pocket. In contrast, the 'LPDLV' Death-associated protein kinase 1 (DAPK1) epitope binds the Kelch-like protein 20 (KLHL20) as a loose helical turn (Figure 2e) [28]. The differential selectivity across the CRL3 Kelch domains could be attributed to variable length of loops at the top of the propeller and differences in patterns of hydrophobic and charged

Figure 2

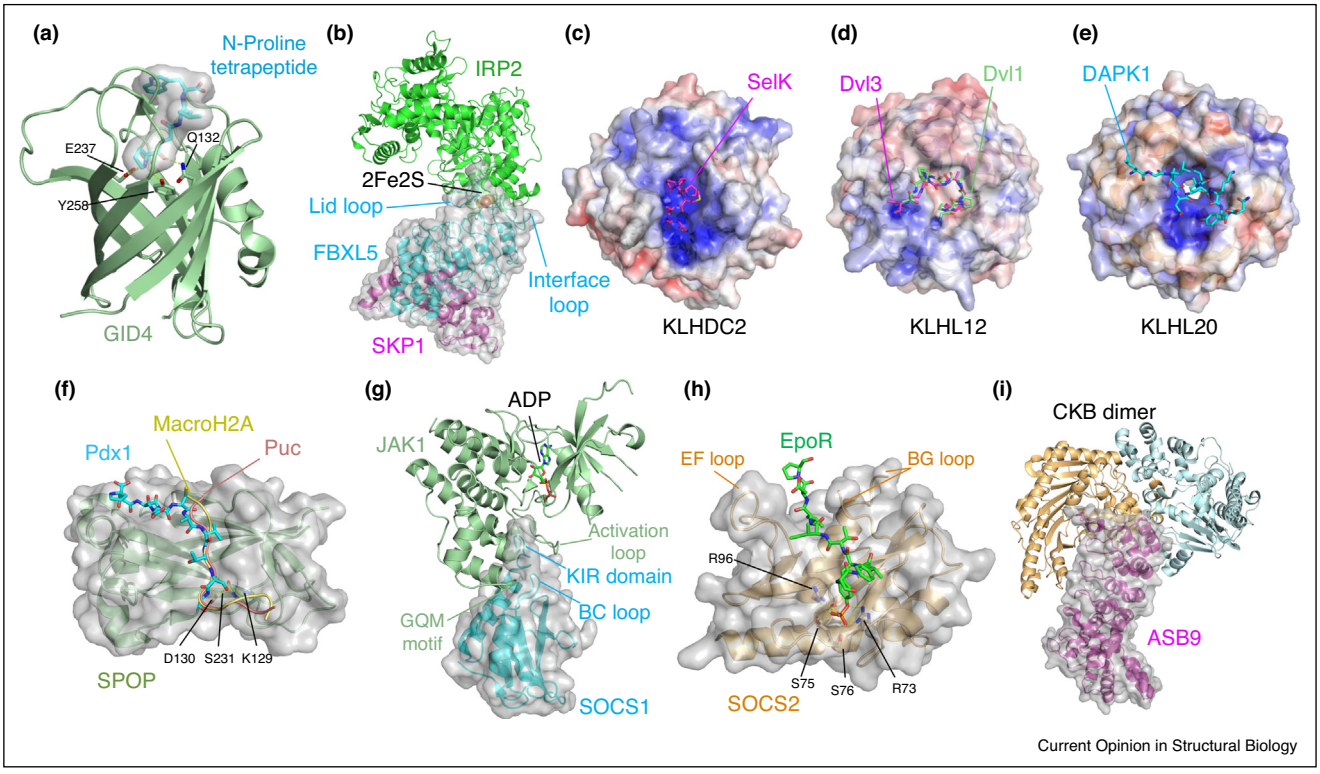

Substrate recognition by E3 ligase substrate receptors: **(a)** GID4 (pale green cartoon) antiparallel β-barrel loops form a narrow groove to recognise N-Proline peptide (cyan carbon sticks) shown as surface (PDB: 6CDC [19•]). **(b)** SKP1 (magenta) and FBXL5 (cyan) of CRL1^{FBXL5} represented in cartoon and transparent surface, interacting with substrate iron response protein 2 (IRP2, green cartoon). Cofactor 2Fe2S, depicted in spheres, mediates the interaction between the FBXL5 leucine rich repeat (LRR) domain and IRP2 domain IV (PDB: 6VCD [23•]). **(c–e)** Electrostatic surface potential map (positive in blue and negative in red) of Kelch repeat domains in complex with substrate degron peptides, shown in sticks. **(c)** SelK (magenta) C-terminus forming a helix and fitting into the positively charged groove of KLHDC2 (PDB: 6DO3 [24]). **(d)** Dvl3 (magenta) and Dvl1 (green) peptides display similar U-turn conformations while interacting with the hydrophobic pocket of KLHL12 (PDB: 6V7O [26], 6TTK [27]). **(e)** DAPK1 (cyan) forming a loose helical turn while interacting with KLHL20 (PDB: 6GY5 [28]). **(f)** Surface view of SPOP MATH domain (pale green cartoon) bound to substrates Pdx1 (cyan carbon sticks), MacroH2A (yellow ribbon) and Puc (wheat ribbon) (PDB: 6F8F [29], 3IVB and 3IVV [30], respectively). **(g)** Kinase inhibitory region (KIR) domain of SOCS1 (cyan cartoon) interacting with JAK1 (pale green cartoon) substrate binding groove (PDB: 6C7Y [31•]). **(h)** Surface view of SOCS2 (light orange) SH2 domain bound with erythropoietin receptor (EpoR) degron peptide (green carbon sticks) (PDB: 6I4X [32•]). **(i)** Surface view of ASB9 (magenta cartoon) in complex with CKB dimer (light orange and light blue cartoon) (PDB: 6V9H [34•]).

residues. Speckle-type POZ protein (SPOP) is an example of CRL3 substrate receptor protein that utilises MATH domain to bind its substrates. The cocrystal structure of pancreas/duodenum homeobox protein 1 (Pdx1) bound to SPOP-MATH relaxes the consensus binding motif for previously characterized SPOP ligands Puc phosphatase and MacroH2A (Φ-p-S-S/T-S/T, Φ:nonpolar; p: polar) to (Φ-p-S-p-p) (Figure 2f) [29,30].

CRL5 substrate-bound structures of suppressor of cytokine signaling 1 (SOCS1), suppressor of cytokine signaling 2 (SOCS2) and ankyrin repeat and SOCS box protein 9 (ASB9) substrate recognition modules have been recently solved. SOCS1 and SOCS2 share a similar domain architecture comprising of an N-terminal extended SH2 subdomain (ESS), a central Src-homology 2 (SH2) domain that recognises a phosphotyrosine (pY) containing sequence, and SOCS box that interacts with the adaptor ElonginB-ElonginC complex (EloBC). The ability of SOCS1 to recruit Cul5 and function as an E3 ligase is compromised because of alterations in the Cullin binding region of its SOCS box. An additional kinase inhibitory region (KIR) domain helps SOCS1 inhibit Janus kinase (JAK1 and JAK2) catalytic activity by blocking its substrate binding groove (Figure 2g) [31•]. Interactions between JAK 'GQM' motif and BC loop of SOCS1 SH2 domain further augments binding affinity. SOCS2 utilises the SH2 domain to recognise phosphodegrons from erythropoietin receptor (EpoR) and growth hormone receptor (GHR) (Figure 2h) [32•]. Unlike in SOCS3 and SOCS6 where the BG loop closes-in over the substrate to form a hydrophobic channel, the loop in

SOCS2 adopts an open conformation that accommodates a wider range of lower-affinity substrates. ASB9 belongs to the largest family of SOCS box containing receptors, with ankyrin repeats serving as the recognition module [33]. A cryo-EM structure of ASB9 bound to the homodimer of Creatine Kinase brain type (CKB) substrate reveals that $ASB9_{25–34}$ form a helix-turn that inserts into a pocket formed by acidic D32 and basic residues (R132, N286, R292, R341) at the interface of the CKB homodimer (Figure 2i) [34•].

Small-molecule glues of E3 ligase:*neo*-substrate interactions

Molecular glues mediate *de novo* PPIs between an E3 ligase and a *neo*-substrate protein leading to polyubiquitination and subsequent degradation of that protein. A first notable example of E3-ligase directed molecular glues is the plant hormone auxin that mediates $CRL1^{TIR1}$-mediated degradation of transcription repressors [35]. Prominent examples of non-natural molecular glues are thalidomide and its Immunomodulatory drugs (IMiDs) analogues lenalidomide and pomalidomide. IMiDs bind to $CRL4^{CRBN}$ and subsequently 'glue' lymphoid transcription factors Ikaros and Aiolos as *neo*-substrates, leading to their proteasomal degradation [36–38]. Crystal structures of DNA damage-binding protein 1 (DDB1)–cereblon (CRBN) complex bound to IMiDs and either casein kinase (CK1α) or G1 to S Phase Transition 1 (GSPT1) as *neo*-substrates provided structural insights into the mechanism of IMiD-mediated modulation of CRBN substrate specificity [36,39]. Recent complex structures of CRBN and pomalidomide with the second zinc finger (ZF2) of Ikaros (IKZF1), zinc finger protein 692(ZNF692) ZF4, and spalt like transcription factor 4 (SALL4) ZF2 highlight that in spite of minimal sequence conservation in the zinc finger degrons, pomalidomide can mediate a conserved binding mode [40•,41•]. An overlay of the complex structures highlight how a strictly conserved glycine of the ZF β-hairpin loop degron docks into a binding hotspot at the CRBN-pomalidomide interface (Figure 3a). These structural insights can now guide the rational design of higher-affinity CRBN binders, including molecular glues with enhanced potency and specificity for improved degradation of neo-substrate proteins [42].

Molecular glues have also been purposefully developed to enhance native E3 ligase-substrate PPIs, otherwise weakened in disease state, for example, as a result of mutations, thus rescuing impaired degradation of substrate protein [43]. The phosphodegron (DpSGφXpS) of oncogenic transcription factor β-catenin is recognised by $CRL1^{β\text{-}TrCP}$ via phosphorylated Ser33 and Ser37, leading to efficient $CRL1^{β\text{-}TrCP}$-dependent ubiquitination and degradation of β-catenin. In many cancers, this PPI is significantly weakened as a result of mutations, for example, Ser-to-Ala or decreased phosphorylation levels — suggesting a strategy for rescuing the PPI via a small-molecular glue approach. Focused screening for enhanced PPI, followed by structure-guided design, achieved molecular glue NRX-2663 that enhanced the binding affinity of unphosphorylated Ser33/S37A β-catenin for β-TrCP by >10 000-fold. Ternary complex structure of NRX-2663 with monophosphorylated pSer33 β-catenin peptide and β-TrCP/Skp1 reveals that a portion of NRX-2663 fills the space left by unphosphorylated Ser37, thus substituting for the missing phosphate group (Figure 3b) [43].

Aryl-sulfonamide (e.g. indisulam) anticancer drugs were found to function as molecular glues to the CRL4 substrate receptor DDB1-associated and CUL4-associated factor 15 (DCAF15), leading to ubiquitination and proteasomal degradation of splicing factor RNA Binding Motif Protein 39 (RBM39), via a mechanism akin to that of IMiDs [44,45]. The structural basis of sulfonamide mode of action was recently elucidated in three independent structural-biophysical studies of sulfonamide-mediated complexes between DDB1–DCAF15 and RBM39 (Figure 3c) [46••,47••,48••]. Indisulam and sulfonamide analogues occupy a shallow groove at the interface between the C-terminal and N-terminal domains of DCAF15, with the two sulfonyl oxygens forming hydrogen bonds with the backbone amide nitrogens of DCAF15 A234 and F235. In addition, the indole nitrogen and sulfonamide nitrogen form extensive water-mediated hydrogen bonds with the side-chain oxygens of RBM39 T262 and D264 (Figure 3c).

Unlike traditional molecular glues that bind to the substrate receptor subunit/domain of E3 ligases, a new class of glue-like compounds recruit E3 ligase machineries once bound to their target protein. The protein kinase inhibitor CR8 was shown to mediate binding of its target cyclin-dependent kinase 12 (CDK12) and the associated partner protein CyclinK to the CRL4 adaptor subunit DDB1. As a result, CDK12 acts as a *neo* substrate-recognition subunit (Figure 3d) [49••]. CDK12 forms extensive interactions with BPA, BPC and C-terminal domains of DDB1, occupying the same position in the assembly as that of a substrate-recognition subunit. Similar to the N-terminus of DCAF15, the C-terminal tail of CDK12 binds to the cleft between the BPA and BPC domains of DDB1. Cyclin K, which binds CDK12 on the opposite side of CDK12, does not contact DDB1 and is presented as a *neo*-substrate, suitably positioned for ubiquitination and subsequent degradation (Figure 3d). More recently, Mayor-Ruiz *et al.* performed a focused compound screening in wild type versus isogenic hyponeddylated cells as an approach to enrich for hits that require functional ubiquitination machineries for their cellular activity [50]. Their screenings identified small molecules that glued between CDKs and DDB1, despite being chemically diverse to CR8.

Figure 3

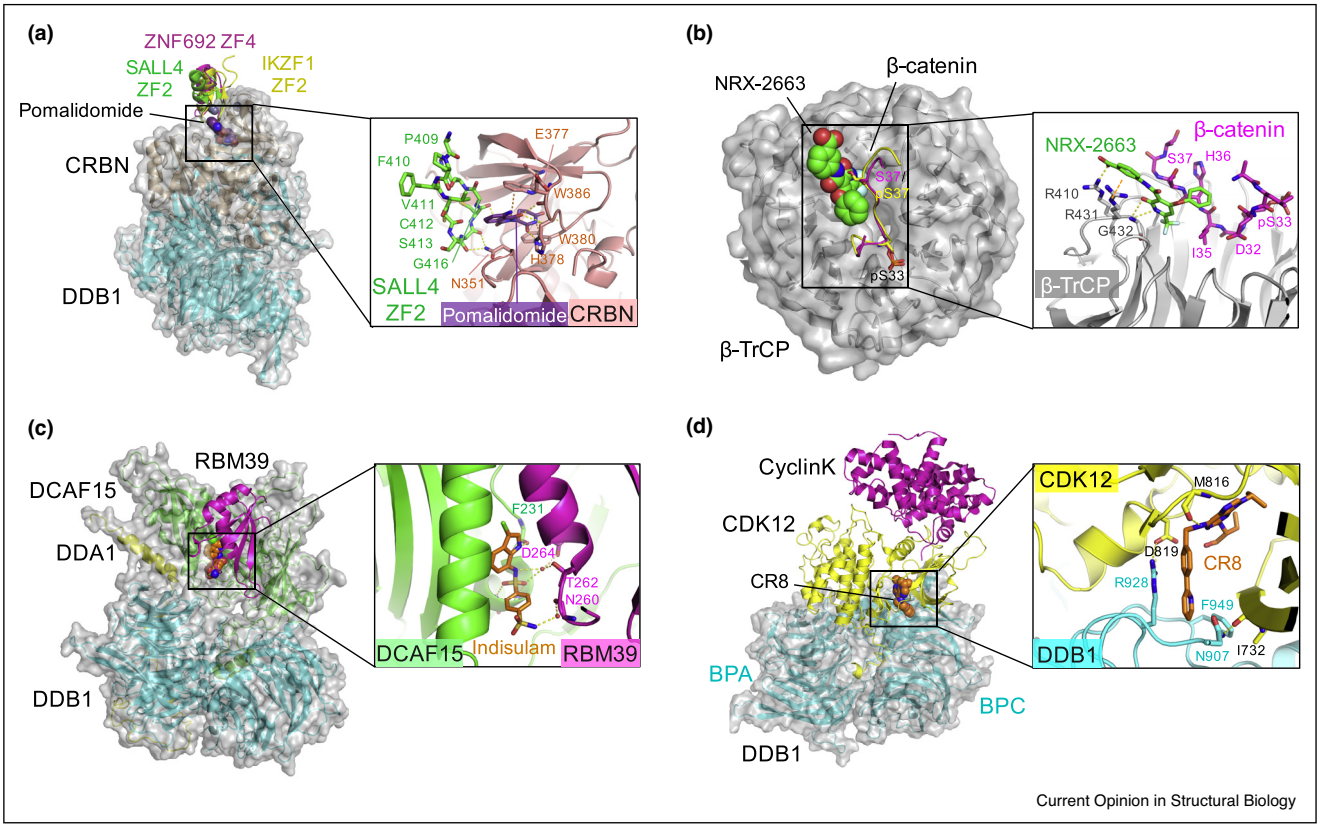

Ternary complexes of E3 ligases with molecular glue degraders: (a–d) E3 ligase is displayed as 40% transparent surface and cartoon representation; substrate is displayed as cartoon and molecular glue is shown as spheres. Zoomed section of the interaction interface shows molecular glue in sticks with key hydrogen bond and cation-π interactions shown in yellow and orange dashed lines, respectively. **(a)** Superposed crystal structures of CRBN(wheat)–DDB1(cyan)–pomalidomide(purple blue carbons) bound to IKZF1 ZF2 (yellow), ZNF692 ZF4 (magenta) and SALL4 ZF2 (green) (PDB: 6H0F [40•], 6H0G [40•], 6UML [41•]). Alignment of structures is performed along the CRBN-CTD. Zoomed section of the interaction interface shows the hairpin loop of the SALL4 ZF2, pomalidomide and interacting residues from CRBN in sticks. **(b)** Ternary complex of β-TrCP (grey), monophosphorylated β-catenin degron peptide (magenta) and NRX-2663 (green carbons) (PDB: 6M92 [43]). Doubly phosphorylated β-catenin peptide (yellow) is superposed to highlight the void occupied by NRX-2633 created by the absence of a phosphate group in Ser37 (PDB: 1P22 [62]). Zoomed section displays NRX-2663 and β-catenin shown in sticks. **(c)** Crystal structure of DCAF15(green)–DDB1(cyan)–DDA1 (yellow) in complex with indisulam (orange carbons) and RBM39 (magenta) (PDB: 6UD7 [46••]). Zoomed section shows indisulam interacting residues from RBM39 and DCAF15 in sticks. Water molecules mediating protein-ligand interactions are displayed as small red spheres. **(d)** Crystal structure of CDK12(yellow)–cyclinK(magenta) with bound CR8 (orange carbons) and DDB1 (cyan) (PDB: 6TD3 [49••]). The C-terminal extension of CDK12 docks into a cleft between the DDB1 domains BPA and BPC, in a manner similar to how the DCAF15 N-terminal tail (and other CRL4 substrate receptors) insert in the same cleft. Zoomed section focusing on the interaction interface between DDB1, CR8 and CDK12.

PROTACs: bifunctional small molecules bridging target proteins to E3 ligases

PROteolysis TArgeting Chimeras (PROTACs) are bifunctional degrader molecules made of an E3 ligase ligand and a target protein ligand, joined by a chemical linker [51,52]. PROTACs can bind to E3 ligase or target protein independently (1:1 complex), before inducing proximity between the two proteins in the form of a ternary complex (1:1:1 complex). Because of their chemical nature, PROTACs differentiate from molecular glues, which lack a linker and can bind to one but not the other of the two proteins. For these reasons, PROTACs were thought of working independently of PPIs between the ligase and the targeted protein. This notion has dramatically changed thanks to emerging structural and biophysical insights into PROTAC ternary complexes, revealing PROTACs can also 'glue' E3 ligase and target protein into stable and cooperative ternary complexes.

Our group solved a first PROTAC ternary structure, composed of our previously discovered PROTAC MZ1, a degrader of the Bromodomain and extraterminal domain (BET) protein Brd4, bound to VHL–ElonginC–ElonginB (VCB) and second bromodomain of Brd4 ($Brd4^{BD2}$) (Figure 4a) [53]. The crystal structure revealed

Figure 4

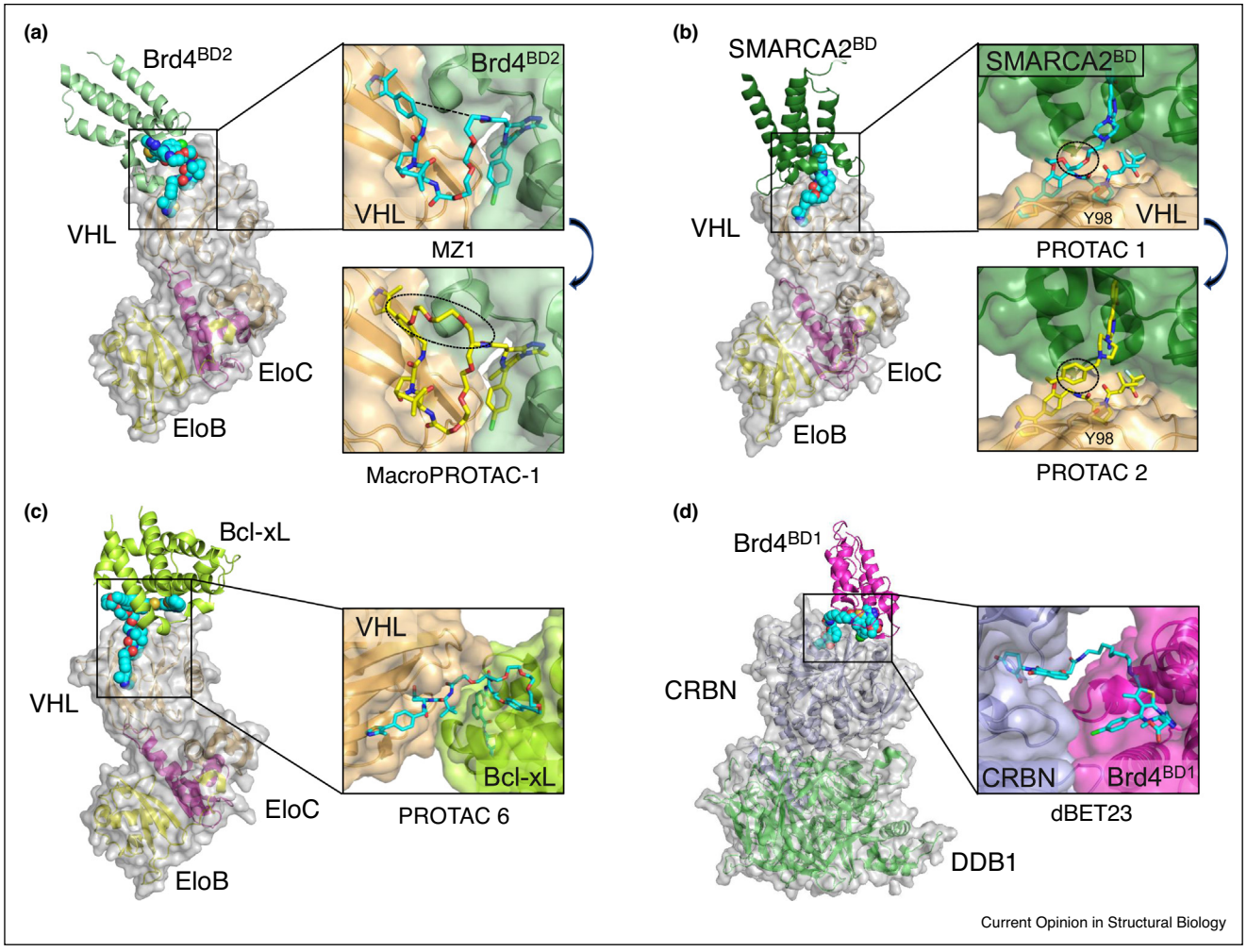

Crystal structures of E3 ligase-PROTAC-Target protein ternary complexes: (a–d) E3 ligase is displayed as 40% transparent surface and cartoon, substrate is displayed as cartoon and PROTAC is shown as spheres. Zoomed section of the interaction interface shows PROTAC in sticks, and surface representation of both E3 ligase and target protein. **(a)** Crystal structure of VHL(orange)-ElonginC(magenta)-ElonginB(yellow) (VCB) in complex with MZ1 (cyan) and Brd4^{BD2} (pale green) (PDB: 5T35 [53]). Zoomed section shows the structure-based rational design of MacroPROTAC-1 (yellow carbon sticks) from MZ1 (PDB: 6SIS [55•]). The bioactive conformation of the linker is locked in MacroPROTAC-1 by cyclising the molecule through linkage of the phenolic group on the VHL ligand and a methylene group adjacent to the BET ligand's amide bond. **(b)** Crystal structure of VCB in complex with PROTAC 1 (cyan) and SMARCA2^{BD} (dark green) (PDB: 6HAY [56••]). Zoomed section shows the structure-based design of PROTAC 2 (PDB: 6HAX [56••]) aimed at rigidifying the linker through substitution of a flexible 5-atom portion of the linker with a phenyl ring. **(c)** Ternary complex of VCB–PROTAC6(cyan)–Bcl-xL(lime green) (PDB: 6ZHC [57•]). **(d)** Crystal structure of CRBN(violet)–DDB1 (green) complex with bound PROTAC dBET23 (cyan) and Brd4^{BD1} (magenta) (PDB: 6BN7 [58]).

non-native *neo*-PPIs between VHL and Brd4^{BD2}, of both hydrophobic and hydrophilic nature, wrapping the PROTAC into a collapsed yet favourable conformation, and resulting in the burial of extensive surface area in the system. The induced PPIs are isoform-specific and contribute to the formation of highly cooperative ($\alpha \sim 20$), stable and long-lived ($t_{1/2} > 2$ min) ternary complex with Brd4^{BD2}, which drive more pronounced ubiquitination and faster degradation of Brd4 in cells [53,54]. With the ternary structure in hand, rational structure-based approaches can be undertaken to design improved PROTAC degraders. On the basis of the MZ1 ternary structure, Gadd *et al.* first designed a novel linkage point and conjugation vector on the VHL binding portion of MZ1, achieving PROTAC degrader AT1 which exhibited improved Brd4-degradation selectivity over MZ1. More recently, Testa *et al.* hypothesized that cyclisation of the PROTAC would lock MZ1 preferentially in its bioactive conformation. Aided by structure-based computational studies, macrocyclic PROTAC degrader MacroPROTAC-1 was designed by adding a cyclizing linker onto MZ1 (Figure 4a). MacroPROTAC-1 showed

degradation activity comparable to MZ1, despite a loss of 12-fold in binding affinity to $Brd4^{BD2}$ [55•].

Another example of successful application of rational structure-based design applied to PROTACs is the development of degraders of SWI/SNF Related, Matrix Associated, Actin Dependent Regulator Of Chromatin, Subfamily A (SMARCA2 and SMARCA4) [56••]. An early, poor degrader of SMARCA2 (PROTAC 1), formed a cooperative ternary complex with VHL ($\alpha \sim 10$) despite its weak (μM) binding affinity for SMARCA2. This observation suggested that high-resolution structure could allow rapid optimization. Ternary complex co-crystal structure revealed extensive *de novo* PPIs contributing favourable binding energy, as in the case of MZ1, however accommodated through an unfavourably collapsed linker. Armed with this information, the linker was rigidified upon replacement of one of its PEG unit with a phenyl group, allowing formation of an additional π-stacking interaction with VHL Y98 (Figure 4b). Further optimization led to potent SMARCA2/4 degrader ACBI1 that formed ternary complexes of improved cooperativity and stability.

Ligase-PROTAC-target complexes have also been solved for systems that do not appear to exhibit positive cooperativity in the ternary equilibria, suggesting avenues for potential optimization strategy. The recent structure of a VCB:PROTAC6:B-cell lymphoma-extra-large (Bcl-xL) complex shows the long PEG linker of PROTAC6 is forced to adopt an extended conformation, before folding back into itself via a compact turn (Figure 4c) [57•]. The unfavourable linker conformational energy likely surpasses any favourable induced PPIs, resulting in the negative cooperativity observed with this system. Relaxing such conformation while maintaining the relative geometry of the ternary complex might lead to improved Bcl-xL PROTAC degraders. Nowak *et al.* structurally characterized non-cooperative ternary complexes formed by CRBN-recruiting JQ1-based PROTACs (dBETs) of varying linker lengths (10–34 atoms) and conjugation points (Figure 4d) [58]. Distinct arrangements of the CRBN–Brd4 interface with different PROTACs highlighted plasticity of the interaction. These structural studies suggest that ternary systems of suboptimal energy and stability may still be productive for targeted protein degradation, if made of high-affinity protein binding ligands.

Conclusions

We have reviewed recent developments in structural understanding of assembly, function and (*neo*)-substrate recognition of E3 ligases. Existence of over 600 E3 ligases in mammalian cells underscore their importance in fine-tuning substrate specificity as a regulatory mechanism of protein homeostasis. E3 ligases are emerging as attractive drug targets in their own right because of their implication and dysregulation in several diseases. Therapeutic exploitation of E3 ligases with small molecules requires a structural and mechanistic understanding of the interplay of protein-protein interactions between their component subunits and how they impart biological function.

For drug development, knowledge of substrate-bound structures of E3 ligases can guide the development of small-molecule inhibitors. The advent of protein degraders that glue to E3 ligases and hijack E3 catalytic activity to effect targeted degradation of intracellular disease-driving proteins are motivating augmented efforts focusing on this family class. Recent years have watched the emergence of structures solved for E3 ligases with molecular glue/PROTAC degraders and *neo*-substrates bound. The structures highlight the growing impact of structural and biophysical understanding of E3 ligase ternary complexes for degrader drug design. These founding advances are motivating current efforts to discover small molecules for more E3 ubiquitin ligases. This has the potential to usher the development of inhibitors or degraders that leverage a wider range of cell-specific, tissue-specific and disease-specific expression as well as functional essentiality and redundancy of E3 ligases, aiding improved therapeutics in the future.

Conflict of interest statement

The Ciulli laboratory receives or has received sponsored research support from Amphista Therapeutics, Boehringer Ingelheim, Eisai, Nurix Therapeutics, and Ono Pharmaceutical. A.C. is a scientific founder, shareholder, director and consultant of Amphista Therapeutics, a company that is developing targeted protein degradation therapeutic platforms.

Acknowledgements

Research in the Ciulli laboratory on E3 ubiquitin ligases and PROTACs receives or has received funding from the European Research Council (ERC, Starting Grant ERC-2012-StG-311460 DrugE3CRLs) and the Innovative Medicines Initiative 2 (IMI2) Joint Undertaking under grant agreement no. 875510 (EUbOPEN project). The IMI2 Join Undertaking receives support from the European Union's Horizon 2020 research and innovation programme, EFPIA companies and Associated Partners: KTH, OICR, Diamond and McGill.

References and recommended reading

Papers of particular interest, published within the period of review, have been highlighted as:

- • of special interest
- •• of outstanding interest

1. Huang X, Dixit VM: **Drugging the undruggables: exploring the ubiquitin system for drug development**. *Cell Res* 2016, **26**:484-498.

2. Komander D, Rape M: **The ubiquitin code**. *Annu Rev Biochem* 2012, **81**:203-229.

3. Zheng N, Shabek N: **Ubiquitin ligases: structure, function, and regulation**. *Annu Rev Biochem* 2017, **86**:129-157.

4. Pao KC, Wood NT, Knebel A, Rafie K, Stanley M, Mabbitt PD, Sundaramoorthy R, Hofmann K, van Aalten DMF, Virdee S:

Activity-based E3 ligase profiling uncovers an E3 ligase with esterification activity. *Nature* 2018, **556**:381-385.

5. Morreale FE, Walden H: **SnapShot: types of ubiquitin ligases**. *Cell* 2016, **165**:248.

6. Weber J, Polo S, Maspero E: **HECT E3 ligases: a tale with multiple facets**. *Front Physiol* 2019, **10**:370.

7. Cotton TR, Lechtenberg BC: **Chain reactions: molecular mechanisms of RBR ubiquitin ligases**. *Biochem Soc Trans* 2020, **48**:1737-1750.

8. Zhong S, Xu Y, Yu C, Zhang X, Li L, Ge H, Ren G, Wang Y, Ma J, Zheng Y *et al.*: **Anaphase-promoting complex/cyclosome regulates RdDM activity by degrading DMS3 in Arabidopsis**. *Proc Natl Acad Sci U S A* 2019, **116**:3899-3908.

9. Barford D: **Structural interconversions of the anaphase-promoting complex/cyclosome (APC/C) regulate cell cycle transitions**. *Curr Opin Struct Biol* 2020, **61**:86-97.

10. Bulatov E, Ciulli A: **Targeting Cullin-RING E3 ubiquitin ligases for drug discovery: structure, assembly and small-molecule modulation**. *Biochem J* 2015, **467**:365-386.

11. Rusnac DV, Zheng N: **Structural biology of CRL ubiquitin ligases**. *Adv Exp Med Biol* 2020, **1217**:9-31.

12. Cardote TAF, Gadd MS, Ciulli A: **Crystal structure of the Cul2-Rbx1-EloBC-VHL ubiquitin ligase complex**. *Structure* 2017, **25** 901–911 e903.

13. •• Baek K, Krist DT, Prabu JR, Hill S, Klugel M, Neumaier LM, von Gronau S, Kleiger G, Schulman BA: **NEDD8 nucleates a multivalent cullin-RING-UBE2D ubiquitin ligation assembly**. *Nature* 2020, **578**:461-466
Illuminates the structural role of NEDD8 in the mechanism of CRL1$^{\beta\text{-TRCP}}$ activation and transfer of ubiquitin from UBE2D to its recruited substrate, phosphorylated IκBα.

14. • Faull SV, Lau AMC, Martens C, Ahdash Z, Hansen K, Yebenes H, Schmidt C, Beuron F, Cronin NB, Morris EP *et al.*: **Structural basis of Cullin 2 RING E3 ligase regulation by the COP9 signalosome**. *Nat Commun* 2019, **10**:3814
Cryo-EM structures of neddylated and deneddylated CSN-CRL2 complexes highlight a conseved mechanism of CSN activity across different CRLs.

15. Cavadini S, Fischer ES, Bunker RD, Potenza A, Lingaraju GM, Goldie KN, Mohamed WI, Faty M, Petzold G, Beckwith RE *et al.*: **Cullin-RING ubiquitin E3 ligase regulation by the COP9 signalosome**. *Nature* 2016, **531**:598-603.

16. Enchev RI, Scott DC, da Fonseca PC, Schreiber A, Monda JK, Schulman BA, Peter M, Morris EP: **Structural basis for a reciprocal regulation between SCF and CSN**. *Cell Rep* 2012, **2**:616-627.

17. • Lin H, Zhang X, Liu L, Fu Q, Zang C, Ding Y, Su Y, Xu Z, He S, Yang X *et al.*: **Basis for metabolite-dependent Cullin-RING ligase deneddylation by the COP9 signalosome**. *Proc Natl Acad Sci U S A* 2020, **117**:4117-4124
Inositol hexakisphosphate (IP6) functions as a CSN cofactor that strengthens CRL–CSN interactions to dislodge the E2 CDC34/UBE2R from CRL, promoting CRL deneddylation.

18. Varshavsky A: **N-degron and C-degron pathways of protein degradation**. *Proc Natl Acad Sci U S A* 2019, **116**:358-366.

19. • Dong C, Zhang H, Li L, Tempel W, Loppnau P, Min J: **Molecular basis of GID4-mediated recognition of degrons for the Pro/N-end rule pathway**. *Nat Chem Biol* 2018, **14**:466-473
First crystal structure of human GID4 in complex with various Pro/N-degrons.

20. Chen SJ, Wu X, Wadas B, Oh JH, Varshavsky A: **An N-end rule pathway that recognizes proline and destroys gluconeogenic enzymes**. *Science* 2017, **355**.

21. •• Qiao S, Langlois CR, Chrustowicz J, Sherpa D, Karayel O, Hansen FM, Beier V, von Gronau S, Bollschweiler D, Schafer T *et al.*: **Interconversion between anticipatory and active GID E3 ubiquitin ligase conformations via metabolically driven substrate receptor assembly**. *Mol Cell* 2020, **77**:150-163
First report on macromolecular assembly of the GID complex. Provides a structural model of transition from inactive anticipatory state to GID4-bound active state in the presence of carbon source.

22. Lucas X, Ciulli A: **Recognition of substrate degrons by E3 ubiquitin ligases and modulation by small-molecule mimicry strategies**. *Curr Opin Struct Biol* 2017, **44**:101-110.

23. • Wang H, Shi H, Rajan M, Canarie ER, Hong S, Simoneschi D, Pagano M, Bush MF, Stoll S, Leibold EA *et al.*: **FBXL5 regulates IRP2 stability in iron homeostasis via an oxygen-responsive [2Fe2S] cluster**. *Mol Cell* 2020, **78** 31–41 e35
Provides structural insight into an iron-sulfur cluster as unprecedented cofactor mediating substrate binding to a CRL, and its role in oxygen sensing.

24. Rusnac DV, Lin HC, Canzani D, Tien KX, Hinds TR, Tsue AF, Bush MF, Yen HS, Zheng N: **Recognition of the diglycine C-end degron by CRL2(KLHDC2) ubiquitin ligase**. *Mol Cell* 2018, **72** 813–822 e814.

25. •• Koren I, Timms RT, Kula T, Xu QK, Li MMZ, Elledge SJ: **The eukaryotic proteome is shaped by E3 ubiquitin ligases targeting C-terminal degrons**. *Cell* 2018, **173**:1622-1635
Identifies multiple C-terminal degrons through global protein stability (GPS) profiling and disclose CRLs that recognise different C-end degrons.

26. Zhao B, Payne WG, Sai JQ, Lu ZW, Olejniczak ET, Fesik SW: **Structural elucidation of peptide binding to KLHL-12, a substrate specific adapter protein in a Cul3-ring E3 ligase complex**. *Biochemistry* 2020, **59**:964-969.

27. Chen Z, Wasney GA, Picaud S, Filippakopoulos P, Vedadi M, D'Angiolella V, Bullock AN: **Identification of a PGXPP degron motif in dishevelled and structural basis for its binding to the E3 ligase KLHL12**. *Open Biol* 2020, **10**:200041.

28. Chen ZY, Picaud S, Filippakopoulos P, D'Angiolella V, Bullock AN: **Structural basis for recruitment of DAPK1 to the KLHL20 E3 ligase**. *Structure* 2019, **27**:1395-1404.

29. Ostertag MS, Messias AC, Sattler M, Popowicz GM: **The structure of the SPOP-Pdx1 interface reveals insights into the phosphorylation-dependent binding regulation**. *Structure* 2019, **27**:327-334.

30. Zhuang M, Calabrese MF, Liu J, Waddell MB, Nourse A, Hammel M, Miller DJ, Walden H, Duda DM, Seyedin SN *et al.*: **Structures of SPOP-substrate complexes: insights into molecular architectures of BTB-Cul3 ubiquitin ligases**. *Mol Cell* 2009, **36**:39-50.

31. • Liau NPD, Laktyushin A, Lucet IS, Murphy JM, Yao S, Whitlock E, Callaghan K, Nicola NA, Kershaw NJ, Babon JJ: **The molecular basis of JAK/STAT inhibition by SOCS1**. *Nat Commun* 2018, **9.1**:1-14
Reports the structural characterisation of JAK1 inhibition by kinase inhibitory region (KIR) of SOCS1.

32. • Kung WW, Ramachandran S, Makukhin N, Bruno E, Ciulli A: **Structural insights into substrate recognition by the SOCS2 E3 ubiquitin ligase**. *Nat Commun* 2019, **10.1**:1-14
First structures of the CRL5 components SOCS2-EloB-EloC in complex with the phosphodegrons derived of its substrates growth hormone receptor and erythropoietin receptor.

33. Thomas JC, Matak-Vinkovic D, Van Molle I, Ciulli A: **Multimeric complexes among ankyrin-repeat and SOCS-box protein 9 (ASB9), ElonginBC, and Cullin 5: insights into the structure and assembly of ECS-type cullin-RING E3 ubiquitin ligases**. *Biochemistry* 2013, **52**:5236-5246.

34. • Lumpkin RJ, Baker RW, Leschziner AE, Komives EA: **Structure and dynamics of the ASB9 CUL-RING E3 ligase**. *Nat Commun* 2020, **11**:2866
Reports the cryo-EM structure of the CRL5 components ASB9-EloB-EloC bound to creatine kinase (CKB) substrate.

35. Tan X, Calderon-Villalobos LI, Sharon M, Zheng C, Robinson CV, Estelle M, Zheng N: **Mechanism of auxin perception by the TIR1 ubiquitin ligase**. *Nature* 2007, **446**:640-645.

36. Petzold G, Fischer ES, Thoma NH: **Structural basis of lenalidomide-induced CK1alpha degradation by the CRL4 (CRBN) ubiquitin ligase**. *Nature* 2016, **532**:127-130.

37. Lu G, Middleton RE, Sun H, Naniong M, Ott CJ, Mitsiades CS, Wong KK, Bradner JE, Kaelin WG Jr: **The myeloma drug lenalidomide promotes the cereblon-dependent destruction of Ikaros proteins**. *Science* 2014, **343**:305-309.

38. Kronke J, Udeshi ND, Narla A, Grauman P, Hurst SN, McConkey M, Svinkina T, Heckl D, Comer E, Li XY *et al.*: **Lenalidomide causes selective degradation of IKZF1 and IKZF3 in multiple myeloma cells**. *Science* 2014, **343**:301-305.

39. Matyskiela ME, Lu G, Ito T, Pagarigan B, Lu CC, Miller K, Fang W, Wang NY, Nguyen D, Houston J *et al.*: **A novel cereblon modulator recruits GSPT1 to the CRL4(CRBN) ubiquitin ligase**. *Nature* 2016, **535**:252-257.

40. • Sievers QL, Petzold G, Bunker RD, Renneville A, Slabicki M, Liddicoat BJ, Abdulrahman W, Mikkelsen T, Ebert BL, Thoma NH: **Defining the human C2H2 zinc finger degrome targeted by thalidomide analogs through CRBN**. *Science* 2018, **362**:558-566

A degradation screen of multiple Cys2-His2 zinc fingers in the presence of IMiDs highlight how diverse amino acid sequences bind the same drug-CRBN interface.

41. • Matyskiela ME, Clayton T, Zheng X, Mayne C, Tran E, Carpenter A, Pagarigan B, McDonald J, Rolfe M, Hamann LG *et al.*: **Crystal structure of the SALL4-pomalidomide-cereblon-DDB1 complex**. *Nat Struct Mol Biol* 2020, **27**:319-322

Crystal structure of SALL4-pomalidomide-CRBN-DDB1 complex reveals the structural basis for the recruitment of neo-substrate SALL4, a potential thalidomide teratogenicity target, to cereblon.

42. Matyskiela ME, Zhang W, Man HW, Muller G, Khambatta G, Baculi F, Hickman M, LeBrun L, Pagarigan B, Carmel G *et al.*: **A cereblon modulator (CC-220) with improved degradation of ikaros and aiolos**. *J Med Chem* 2018, **61**:535-542.

43. Simonetta KR, Taygerly J, Boyle K, Basham SE, Padovani C, Lou Y, Cummins TJ, Yung SL, von Soly SK, Kayser F *et al.*: **Prospective discovery of small molecule enhancers of an E3 ligase-substrate interaction**. *Nat Commun* 2019, **10.1**:1-12.

44. Han T: **Anticancer sulfonamides target splicing by inducing RBM39 degradation via recruitment to DCAF15 (vol 356, eaan7977, 2017)**. *Science* 2017, **357**:143.

45. Uehara T, Minoshima Y, Sagane K, Sugi NH, Mitsuhashi KO, Yamamoto N, Kamiyama H, Takahashi K, Kotake Y, Uesugi M *et al.*: **Selective degradation of splicing factor CAPERalpha by anticancer sulfonamides**. *Nat Chem Biol* 2017, **13**:675-680.

46. •• Bussiere DE, Xie LL, Srinivas H, Shu W, Burke A, Be C, Zhao JP, Godbole A, King D, Karki RG *et al.*: **Structural basis of indisulam-mediated RBM39 recruitment to DCAF15 E3 ligase complex (vol 16, pg 15, 2019)**. *Nat Chem Biol* 2020, **16**:361

This is one of the three parallel articles reporting the structural basis of indisulam sulfonamides gluing activity to CRL4 DCAF15 to mediate RBM39 degradation.

47. •• Faust TB, Yoon H, Nowak RP, Donovan KA, Li Z, Cai Q, Eleuteri NA, Zhang T, Gray NS, Fischer ES: **Structural complementarity facilitates E7820-mediated degradation of RBM39 by DCAF15**. *Nat Chem Biol* 2020, **16**:7-14

This is one of the three parallel articles reporting the structural basis of indisulam sulfonamides gluing activity to CRL4 DCAF15 to mediate RBM39 degradation.

48. •• Du XL, Volkov OA, Czerwinski RM, Tan HL, Huerta C, Morton ER, Rizzi JP, Wehn PM, Xu R, Nijhawan D *et al.*: **Structural basis and kinetic pathway of RBM39 recruitment to DCAF15 by a sulfonamide molecular glue E7820**. *Structure* 2019, **27**:1625-1633

This is one of the three parallel articles reporting the structural basis of indisulam sulfonamides gluing activity to CRL4 DCAF15 to mediate RBM39 degradation.

49. •• Slabicki M, Kozicka Z, Petzold G, Li YD, Manojkumar M, Bunker RD, Donovan KA, Sievers QL, Koeppel J, Suchyta D *et al.*: **The CDK inhibitor CR8 acts as a molecular glue degrader that depletes cyclin K**. *Nature* 2020, **585**:293-297

First report of a molecular glue targeting the CRL adaptor subunit DDB1 instead of the substrate receptor subunit, when in complex with its target protein.

50. Mayor-Ruiz C, Bauer S, Brand M, Kozicka Z, Siklos M, Imrichova H, Kaltheuner IH, Hahn E, Seiler K, Koren A *et al.*: **Rational discovery of molecular glue degraders via scalable chemical profiling**. *Nat Chem Biol* 2020, **16**:1199-1207.

51. Maniaci C, Ciulli A: **Bifunctional chemical probes inducing protein-protein interactions**. *Curr Opin Chem Biol* 2019, **52**:145-156.

52. Burslem GM, Crews CM: **Proteolysis-targeting chimeras as therapeutics and tools for biological discovery**. *Cell* 2020, **181**:102-114.

53. Gadd MS, Testa A, Lucas X, Chan KH, Chen WZ, Lamont DJ, Zengerle M, Ciulli A: **Structural basis of PROTAC cooperative recognition for selective protein degradation**. *Nat Chem Biol* 2017, **13**:514-521.

54. Roy MJ, Winkler S, Hughes SJ, Whitworth C, Galant M, Farnaby W, Rumpel K, Ciulli A: **SPR-measured dissociation kinetics of PROTAC ternary complexes influence target degradation rate**. *ACS Chem Biol* 2019, **14**:361-368.

55. • Testa A, Hughes SJ, Lucas X, Wright JE, Ciulli A: **Structure-based design of a macrocyclic PROTAC**. *Angew Chem Int Ed* 2020, **59**:1727-1734

Reports the structure-based design of a first macrocyclic PROTAC as an approach to constrain the degrader molecule its bioactive confirmation.

56. •• Farnaby W, Koegl M, Roy MJ, Whitworth C, Diers E, Trainor N, Zollman D, Steurer S, Karolyi-Oezguer J, Riedmueller C *et al.*: **BAF complex vulnerabilities in cancer demonstrated via structure-based PROTAC design (vol 15, pg 672, 2019)**. *Nat Chem Biol* 2019, **15**:846

An elegant example of using PROTAC ternary complex crystal structures to design potent degraders for the chromatin remodelling complex BAF subunits SMARCA2 and SMARCA4.

57. • Chung CW, Dai H, Fernandez E, Tinworth CP, Churcher I, Cryan J, Denyer J, Harling JD, Konopacka A, Queisser MA *et al.*: **Structural insights into PROTAC-mediated degradation of Bcl-xL**. *ACS Chem Biol* 2020, **15**:2316-2323

Crystal structure of Bcl-xL:PROTAC:VHL-ElonginB-ElonginC as an example of structural characterization of low-cooperativity complexes.

58. Nowak RP, DeAngelo SL, Buckley D, He ZX, Donovan KA, An J, Safaee N, Jedrychowski MP, Ponthier CM, Ishoey M *et al.*: **Plasticity in binding confers selectivity in ligand-induced protein degradation**. *Nat Chem Biol* 2018, **14**:706-714.

59. Goldenberg SJ, Cascio TC, Shumway SD, Garbutt KC, Liu JD, Xiong Y, Zheng N: **Structure of the Cand1-Cul1-Roc1 complex reveals regulatory mechanisms for the assembly of the multisubunit cullin-dependent ubiquitin ligases**. *Cell* 2004, **119**:517-528.

60. Fischer ES, Scrima A, Bohm K, Matsumoto S, Lingaraju GM, Faty M, Yasuda T, Cavadini S, Wakasugi M, Hanaoka F *et al.*: **The molecular basis of CRL4(DDB2/CSA) ubiquitin ligase architecture, targeting, and activation**. *Cell* 2011, **147**:1024-1039.

61. Stebbins CE, Kaelin WG, Pavletich NP: **Structure of the VHL-ElonginC-ElonginB complex: implications for VHL tumor suppressor function**. *Science* 1999, **284**:455-461.

62. Wu G, Xu GZ, Schulman BA, Jeffrey PD, Harper JW, Pavletich NP: **Structure of a beta-TrCP1-Skp1-beta-catenin complex: destruction motif binding and lysine specificity of the SCF beta-TrCP1 ubiquitin ligase**. *Mol Cell* 2003, **11**:1445-1456.